Research article

JGS
Journal of the Geological Society

https://doi.org/10.1144/jgs2020-035 | Vol. 178 | 2021 | jgs2020-035

Paleozoic crustal evolution and tectonic switching in the Northeastern Tianshan: insights from zircon Hf isotopes of granitoids

Long Du[1,2,3], Hongli Zhu[2,4], Chao Yuan[5], Yunying Zhang[6], Zongying Huang[5], Xu-Ping Li[1] and Xiaoping Long[3*]

[1] College of Earth Science and Engineering, Shandong University of Science and Technology, Qingdao 266590, China
[2] Laboratory for Marine Mineral Resources, Qingdao National Laboratory for Marine Science and Technology, Qingdao 266237, China
[3] State Key Laboratory of Continental Dynamics, Department of Geology, Northwest University, Xi'an 710069, China
[4] Center of Deep Sea Research, Institute of Oceanography, Chinese Academy of Sciences, Qingdao 266071, China
[5] State Key Laboratory of Isotope Geochemistry, Guangzhou Institute of Geochemistry, Chinese Academy of Sciences, Guangzhou 510640, China
[6] Department of Earth Sciences, The University of Hong Kong, Hong Kong, China
XL, 0000-0003-0996-196X
*Correspondence: longxp@nwu.edu.cn

Decoding the crustal and tectonic evolution of ancient accretionary orogens is not always straightforward. Here, four episodes of Paleozoic granitoids have been identified with distinct zircon–Hf isotopic characteristics from the Northeastern Tianshan. The first stage granitoids in the Dananhu–Harlik arc system are characterized by highly positive zircon $\varepsilon_{Hf}(t)$ values and short crustal incubation times with a rising event signature, suggesting a northward trench advance for the Kangguer Ocean. During the second stage, granitoids in the Dananhu and Kangguer belts have high zircon $\varepsilon_{Hf}(t)$ values and short crustal incubation times, but with a decreasing event signature for the Dananhu granitoids, implying a reworking of the juvenile arc crust. However, the near-zero $\varepsilon_{Hf}(t)$ values and the longest crustal incubation times of the Yamansu granitoids in this stage elucidate an origin from a Precambrian basement. These variations suggest that the northern trench of the Kangguer Ocean retreated southward while the southern trench advanced southward. During the third stage, the enlarged ranges of zircon $\varepsilon_{Hf}(t)$ values and crustal residence ages as well as crustal incubation times for the Dananhu and Kangguer granitoids show an interaction of juvenile material and the pre-existing crust, whereas the highly positive zircon $\varepsilon_{Hf}(t)$ values with a sharp rising event signature of the Yamansu granitoids suggest an significant crustal growth, indicating that a northward trench advance and a southern trench retreat for the Kangguer Ocean. However, the last stage granitoids in the Northeastern Tianshan entirely exhibit decreasing zircon $\varepsilon_{Hf}(t)$ values and long crustal incubation times, demonstrating a reworking of the pre-existing juvenile crust with minor input of ancient crustal materials in a post-collisional setting.

Supplementary material: Table S1 and S2 and analytical methods are available at https://doi.org/10.6084/m9.figshare.c.5197889

Received 20 February 2020; revised 28 September 2020; accepted 4 November 2020

Accretionary orogenic belts generally occur along convergent plate margins in which deformation, metamorphism and crustal growth took place as a consequence of continuing subduction and accretion (Beltrando et al. 2007; Cawood et al. 2009). They can be grouped into advancing and retreating endmember types, based on the motion of the overriding plate relative to the downgoing plate, which show a distinct crustal structure and tectonic environment (Collins 2002; Cawood et al. 2009). Trench advance is characterized by the overriding plate advances towards the downgoing slab, inducing crustal thickening and enhanced crustal materials being added into the mantle (Collins 2002; Cawood et al. 2009), whereas trench retreat is marked by the downgoing slab moving away from the overriding plate, resulting in crustal thinning and arc splitting in the upper plate (Collins 2002; Cawood et al. 2009). Over the course of geological history, tectonic switching between phases of trench advance and retreat have frequently occurred rather than solely advancing or retreating accretionary orogen (e.g. Collins 2002; Beltrando et al. 2007). Geophysical investigations are very useful in providing information on the crustal structure and tectonic setting of modern accretionary orogenic belts (McKenzie and Priestley 2008; Royden et al. 2008). However, due to the lack of geological and geodynamical evidence, recognition of trench advance and retreat in ancient accretionary orogenic belts is not always straightforward (Zhang et al. 2018, 2019).

With the rapid improvements in analytical techniques, in combination with in situ zircon U–Pb dating and Lu–Hf isotope analysis of granitoid rocks from ancient island arcs or back-arc basins, it has been possible to unravel the nature, crust architecture and tectonic evolution of ancient accretionary orogenic belts (Kinny and Maas 2003; Kemp et al. 2006; Glen et al. 2011; Zhang et al. 2018; Wang et al. 2019). Zircons are abundant in granitoid rocks, and can not only provide precise crystallization ages of the parental magmas, but also essentially preserve the initial $^{176}Hf/^{177}Hf$ ratios on account of their extremely low Lu/Hf ratios, providing a perfect record of the Hf isotopic compositions of the host magmas at the time of zircon crystallization (Kinny and Maas 2003; Zhu et al. 2011; Zhang et al. 2019). Importantly, their stable physicochemical characteristics allow zircons to survive from subsequent multiple geological events (Kinny and Maas 2003; Zhu et al. 2011; Zhang et al. 2019), such as crustal anatexis (Tang et al. 2014), (ultra-)

high-pressure metamorphism (Zheng et al. 2005), and zircon recrystallization, alteration or overgrowth (Gerdes and Zeh 2009). Additionally, Hf isotopic compositions of zircon are primarily controlled by the nature of magma sources (Smith et al. 1987; Kinny and Maas 2003) and have thus become a powerful tracer for studying crustal evolution (Kemp et al. 2006; Scherer et al. 2007); also, long-term Hf-in-zircon variations have succeeded in discriminating accretionary orogenic belt histories (e.g. Collins et al. 2011; Boekhout et al. 2013).

As the largest Phanerozoic accretionary orogenic belt in the world, the Central Asian Orogenic Belt (CAOB) is characterized by multiple accretion of various terranes, such as island arcs, ophiolites, accretionary prisms, and possibly some microcontinents (Sengör et al. 1993; Windley et al. 2007; Xiao et al. 2015). Some scholars have proposed that at least half of its crustal growth was due to the addition of juvenile material during the Neoproterozoic and Paleozoic (e.g. Sengör et al. 1993; Jahn et al. 2004; Tang et al. 2017). Others have argued that the production of mantle-derived or juvenile continental crust during the accretionary history of the CAOB has been grossly overestimated (Kröner et al. 2014, 2017). As one of the main mountain ranges of the CAOB, the Chinese Tianshan was formed by Paleozoic multiple subduction and accretion, and probably experienced episodic trench advance and retreat (e.g. Xiao et al. 2004; Zhang et al. 2018). The Chinese Tianshan is made up of a series of island arc assemblages, remnants of oceanic crust, accretionary wedges and microcontinents (e.g. Windley et al. 2007; Xiao et al. 2015). Among the island arc assemblages in the Chinese Tianshan, the Northeastern Tianshan is characterized by two major island arc assemblages: the Dananu–Harlik arc in the north, and the Yamansu arc in the south, separated by the Kangguer suture zone, with a vast expanse of Paleozoic granitoid rocks that are characterized by positive $\varepsilon_{Nd}(t)$ and $\varepsilon_{Hf}(t)$ values (e.g. Jahn et al. 2004; Xiao et al. 2004; Tang et al. 2017; Zhang et al. 2018). This provides an ideal opportunity for us to study the trench advance and retreat history, as well as to assess the crustal evolution in an ancient accretionary orogenic belt.

In this study, we present a systematic in situ U–Pb dating and new Hf isotope analysis on zircons of Paleozoic granitoids from different tectonic units in the Northeastern Tianshan. Based on these new data (reported in Supplementary Data, Table S1), together with the data from the recent literature (the data and references are provided in Supplementary Data, Table S2), we attempt to characterize the geochemical indices of an ancient accretionary orogenic belt and thus to unveil the Paleozoic crustal and tectonic evolutionary histories of the Northeastern Tianshan.

Geological background and sample descriptions

The Chinese Tianshan separates the Junggar basin to the north from the Tarim block to the south (Fig. 1). It can be geographically divided into the Eastern Tianshan and Western Tianshan roughly by 89°E longitude. The Eastern Tianshan further can be tectonically subdivided into the North Tianshan belt, the Central Tianshan block and the South Tianshan belt (Fig. 1b; Xiao et al. 2004; Charvet et al. 2007). The central Eastern Tianshan block predominantly consists of Precambrian metamorphic basement composed of gneissic granitoids (e.g. granodiorite, monzogranite and tonalite), which is overlain by Paleozoic to Mesozoic magmatic and sedimentary rocks (e.g. Hu et al. 2000; Huang et al. 2019). The Southeastern Tianshan belt is dominated by Paleozoic high-pressure metamorphic assemblages, marine sediments, volcaniclastic rocks and relics of ophiolites (Xiao et al. 2004; Charvet et al. 2007).

The Northeastern Tianshan belt comprises the Harlik and Dananhu arcs in the north, and the Yamansu arc in the south, with the Kangguer belt situated between them as a suture zone (Fig. 1c; Xiao et al. 2004; Zhang et al. 2018). The oldest sedimentary strata in the Harlik and Dananhu terranes are the Ordovician to Silurian Huangcaopo Group and Middle Ordovician Daliugou Group, respectively (Ma 1999; Deng et al. 2016). The former are predominantly overlain by Devonian to Carboniferous flysch and clastic sediments, intercalated with minor volcaniclastic and volcanic rocks (Ma 1999). The latter are overlain by Devonian volcanic and pyroclastic rocks (Deng et al. 2016), which are unconformably overlain by Carboniferous to Permian volcanic rocks (Gao et al. 2015). Moreover, the Harlik and Dananhu arcs were characterized by prolonged Ordovician to Carboniferous island arc magmatism (e.g. Du et al. 2018a, 2019a; Zhang et al. 2018; Sun et al. 2019). The Yamansu belt predominantly contains Carboniferous volcanic and pyroclastic rocks, which are dominantly basalt, andesite and pyroclastic rocks (Hou et al. 2014), and were intruded by numerous Late Paleozoic arc-related granitoids (e.g. Zhang et al. 2016; Du et al. 2018b; Zhao et al. 2019a, b). The Kangguer belt extends c. 600 km long with width varying between 5 and 24 km and is envisaged as a suture zone (Xiao et al. 2004; Zhang et al. 2018). This belt is mainly made up of Carboniferous volcanic and sedimentary rocks, with ophiolite fragments locally deposited in the north (Xiao et al. 2004; Wang et al. 2014). With respect to ophiolites, geochemical data suggest their variable suprasubduction zone (SSZ) signatures, which mainly contain meta-basalts, serpentinized peridotites and meta-gabbros, with a Late Cambrian zircon U–Pb age (c. 494 Ma) and an Early Carboniferous zircon U–Pb age (c. 330 Ma) (Li et al. 2008; Liu et al. 2016).

Samples of this study were collected from the Northeastern Tianshan, including a dioritic pluton from the Harlik belt, one dioritic and three granitic plutons from the Dananhu belt, four granitic plutons from the Kangguer belt, and two dioritic and three granitic plutons from the Yamansu belt. For more details on the descriptions of these granitoid samples, see Du et al. (2018a, b, 2019a, b).

Analytical results

Details of the analytical method and results of this study are provided in Supplementary Data: Analytical Method and Table S1. In addition, we collected the available published zircon U–Pb and Lu–Hf isotopic data of Paleozoic granitoids in the Northeastern Tianshan from previous literature, which can be found in Supplementary Data, Table S2.

Samples from the Harlik belt

Zircons from the diorite sample (X3ET405) in the Harlik belt show oscillatory zoning with high Th/U ratios (>0.2), indicating an igneous origin (Belousova et al. 2002; Du et al. 2018a). Twenty grains yielded a U–Pb age of 452 ± 4 Ma (Du et al. 2018a). The spot locations for Lu–Hf isotopes in this study were the same as those for U–Pb analyses. These zircons yielded $^{176}Hf/^{177}Hf$ ratios and $\varepsilon_{Hf}(t)$ values of 0.282840–0.282948 and 12.0–15.8, with corresponding young one-stage model ages (T_{DM}) of 429–585 Ma and two-stage model ages (T_{DM}^{C}) of 418–664 Ma (Table S1).

Samples from the Dananhu belt

All the zircons of granitoids from the Dananhu belt are characterized by high Th/U ratios and well-developed oscillatory zoning, suggesting an igneous origin (Belousova et al. 2002; Du et al. 2018a, 2019a). The zircon grains yielded a U–Pb age of 442 ± 3 Ma for a dioritic pluton (X3ET355), 447 ± 5 Ma for a granitic pluton (X3ET340), 357 ± 3 Ma for a porphyritic granitic pluton (X3ET372), and 311 ± 3 Ma for a K-feldspar granitic pluton (X3ET459) (Du et al. 2018a, 2019a). These zircons show respective $^{176}Hf/^{177}Hf$ ratios of 0.282769–0.282940, 0.282802–0.282937, 0.282852–0.282959 and 0.282797–0.282974

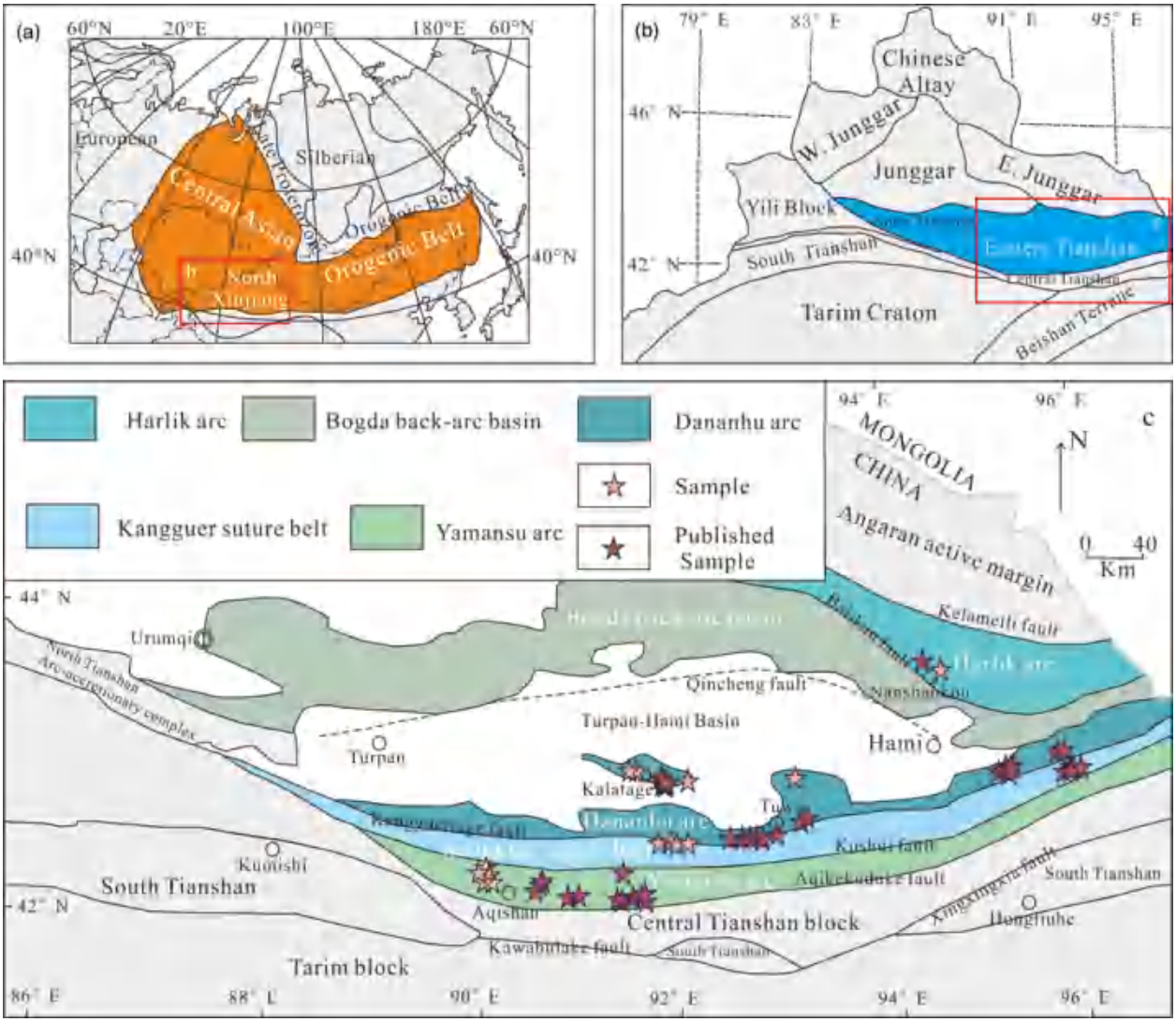

Fig. 1. (a) Simplified geological map of the Central Asian Orogenic Belt (modified from Gao et al. 2011). (b) Simplified geological map of the North Xinjiang (modified from Gao et al. 2009). (c) Geological map of the Eastern Tianshan (modified after Xiao et al. 2004).

(Table S1). They have similar positive $\varepsilon_{Hf}(t)$ values of 8.1–15.4, 9.7–15.3, 10.2–14.1 and 7.1–13.1, with young one-stage model ages (T_{DM} = 442–758 Ma, 451–676 Ma, 425–585 Ma and 413–677 Ma) and two-stage model ages (T^{C}_{DM} = 442–900 Ma, 456–797 Ma, 460–708 Ma and 473–861 Ma) (Table S1).

Samples from the Kangguer belt

Zircons from the Kangguer belt granitoids also show typical characteristics of magmatic zircons (Belousova et al. 2002; Du et al. 2019b). U–Pb dating of these zircons yielded a mean age of 360 ± 3 Ma for a porphyritic granitic intrusion (X3ET239), 317 ± 5 Ma for a porphyritic granodioritic intrusion (X3ET232), 310 ± 2 Ma for a granodioritic porphyry intrusion (X3ET222), and 302 ± 4 Ma for a granodioritic intrusion (X3ET223) (Du et al. 2019b). The dated zircons from these granitoids show corresponding $^{176}Hf/^{177}Hf$ ratios of 0.282872–0.282933, 0.282846–0.282961, 0.282893–0.282987 and 0.282890–0.283011, respectively (Table S1). Similar to zircons from the Harlik and Dananhu granitoids, they have positive $\varepsilon_{Hf}(t)$ values of 11.1–13.3, 8.8–13.7, 10.8–14.4 and 10.6–14.9, with young one-stage model ages (T_{DM} = 449–537 Ma, 410–586 Ma, 370–511 Ma and 348–520 Ma) and two-stage model ages (T^{C}_{DM} = 508–646 Ma, 461–750 Ma, 406–630 Ma and 370–643 Ma) (Table S1).

Samples from the Yamansu belt

Zircons from granitoids in the Yamansu belt show typical characteristics of magmatic zircons (Belousova et al. 2002; Du et al. 2018b). These grains from a granodioritic pluton (X3SS01) and its dioritic enclave (X3SS08) yielded U–Pb ages of 336 ± 3 and 335 ± 2 Ma, respectively (Du et al. 2018b). Moreover, zircon U–Pb dating gave a mean age of 333 ± 3 Ma for an albitophyre sample (X3SS14), 292 ± 3 Ma for a K-feldspar granite sample (X3SS34), and 281 ± 2 Ma for a monzonitic granite sample (X3SS22) (Du et al. 2018b). The corresponding Lu–Hf isotopic analysis of these zircons shows $^{176}Hf/^{177}Hf$ ratios (0.282613–0.282747, 0.282619–0.282755, 0.282591–0.282739, 0.282767–0.282920 and 0.282732–0.282891, respectively) lower than those in the above three tectonic belts (Table S1). They have positive but lower $\varepsilon_{Hf}(t)$ values of 1.3–6.3, 1.1–6.6, 0.7–5.9, 4.8–10.8 and 4.5–10.1, with older one-stage model ages (T_{DM} = 724–927 Ma, 709–990 Ma, 730–944 Ma, 513–848 Ma and 519–748 Ma) and two-stage model ages (T^{C}_{DM} = 943–1255 Ma, 924–1270 Ma, 963–1295 Ma, 616–1003 Ma and 654–1013 Ma) (Table S1).

Discussion

Voluminous Paleozoic granitoids occurred in the Northeastern Tianshan (Tables S1 and S2). They were primarily generated by

partial melting of middle to lower crust, with compositions being controlled by crustal sources (e.g. Du et al. 2018a; Zhao et al. 2019a; Long et al. 2020). Zircon is a common accessory mineral in granitoid rocks, and its Lu–Hf isotopic composition is a powerful tool in tracing the nature of crustal rocks and determining the evolutionary history of crust (Griffin et al. 2004; Kemp et al. 2006; Meng et al. 2019; Song et al. 2019; Xiao et al. 2020). In general, magmatic rocks derived wholly from the depleted mantle exhibit highly positive zircon $\varepsilon_{Hf}(t)$ values, whereas magmatic rocks generated entirely by the reworking of ancient continental crust show negative zircon $\varepsilon_{Hf}(t)$ values, and those formed by magma mixing display large variations in $\varepsilon_{Hf}(t)$ values (Griffin et al. 2004; Kemp et al. 2006). Nevertheless, the use of $\varepsilon_{Hf}(t)$ values in zircons alone cannot effectively distinguish the granitoid rocks that formed by the reworking of the juvenile crust from those that directly origined from the mantle, both of which have positive zircon $\varepsilon_{Hf}(t)$ values.

Single-stage Hf model age (T_{DM}) was calculated based on a depleted-mantle source, and can give a minimum age for the source material of the magma from which the zircon crystallized (Griffin et al. 2006; Belousova et al. 2009). The comparison of large volumes of data on the U–Pb ages plotted against the difference between zircon U–Pb ages and Hf model ages (Age–T_{DM}) can be simplified by reducing the data to 'event signature curves' that illustrate the evolutionary features of the crustal residence age of the source (Griffin et al. 2006; Belousova et al. 2009). These researchers proposed that an increasing trend with decreasing age indicates addition of juvenile materials and a downward trend with decreasing age reflects ancient crustal reworking, while magma mixing between them produces an intermediate slope (Griffin et al. 2006; Belousova et al. 2009). This theory is well supported by magmatic rocks generated by source regions with ancient crust, such as the Mt Isa block in Australia (Griffin et al. 2006), Gawler Craton in Australia (Belousova et al. 2009), and the Central Tianshan block in China (Huang et al. 2019). Considering that neither have ancient crustal basement been reported in previous literature (e.g. Zhang et al. 2018; Sun et al. 2019), nor have magmatic zircons with negative $\varepsilon_{Hf}(t)$ values been found in the Northeastern Tianshan or the Yamansu belt, these samples show a downward trend with decreasing age, unlikely to be caused by ancient crustal reworking, since juvenile material directly input will produce a sharp rising trend with highly positive $\varepsilon_{Hf}(t)$ values. We therefore suggest reworking of ancient crust will create a downward trend with decreasing age and negative $\varepsilon_{Hf}(t)$ values, while reworking of juvenile crust will generate a downward trend with decreasing age with positive but relatively low $\varepsilon_{Hf}(t)$ values.

As most zircons have crystallized from quartz-saturated magma, they were produced by partial melting of the crust through two steps: Hf crustal model ages define step 1, separation of primitive crust from the mantle, and U–Pb ages date step 2, widespread melts of the primitive crust to form granitoids (Wang et al. 2009, 2011). Therefore, 'crustal incubation time' is another crucial indicator in revealing crustal evolution; it is defined as the difference between the Hf crustal model age and zircon U–Pb age (T_{DM}^{C}–Age) (Wang et al. 2009, 2011; Li et al. 2014). Zircons generated by juvenile crustal materials have crustal incubation times less than 300 Ma (Wang et al. 2009,2011), whereas those formed by the reworking of pre-existing ancient crust will result in high crustal incubation times (>300 Ma) (Wang et al. 2009, 2011; Li et al. 2014; Huang et al. 2019). Hence, we also regard a crustal incubation time of 300 Ma as the dividing line between juvenile crust and ancient crust in this study, and assume that a short crustal incubation time (<300 Ma) generally reflects a juvenile material addition, whereas a long crustal incubation time (>300 Ma) implies an ancient crust reworking (Wang et al. 2009, 2011; Li et al. 2014; Huang et al. 2019).

Although a specific tectonic setting does not necessarily produce magmas with a unique Hf isotopic composition of zircons, long-term Hf-in-zircon variations have succeeded in revealing the relative contribution of juvenile and ancient crustal components as well as discriminating trench advance and retreat in accretionary orogens (e.g. Collins et al. 2011; Boekhout et al. 2013; Zhang et al. 2019). Overall, in order to identify the Paleozoic evolutionary characteristics of the Northeastern Tianshan, we comprehensively analyse the zircon $\varepsilon_{Hf}(t)$ values, event signature curves and crustal incubation times of the Paleozoic (c. 470–280 Ma) granitoids in the Harlik, Dananhu, Kangguer, and Yamansu belts (Figs 2–4).

Middle Ordovician to Late Carboniferous crustal evolution and tectonic switching of the Dananhu–Harlik arc system

Recently, the earliest (Middle to Late Ordovician) magmatic rocks in the Northeastern Tianshan have been identified in the Nanshankou area, Harlik belt, and the Kalatage area, Dananhu belt (e.g. Deng et al. 2016; Du et al. 2018a; Sun et al. 2019). The arc-like geochemical features of these Ordovician granitoids demonstrate they were generated in an arc-related tectonic setting (e.g. Deng et al. 2016; Du et al. 2018a; Sun et al. 2019). Since the consistency of the Ordovician to Silurian sedimentary strata and the oldest magmatism occurred both in the Harlik and Dananhu arcs (Ma 1999; Du et al. 2018a), the asymmetrically magmatic distributions in the two arcs during this period indicate that they were probably generated in a single arc system during the Ordovician to Silurian (Zhang et al. 2018). From the combination of the arc-like granitoids, sedimentary strata records, and detailed structural geological studies undertaken in this region, the Harlik and Dananhu arcs were considered to be a united arc system as a consequence of initial northward subduction of the Kangguer ocean since the Middle Ordovician (Du et al. 2018a; Zhang et al. 2018; Sun et al. 2019).

The Middle Ordovician granitoids in both the Harlik and Dananhu belts were characterized by highly positive $\varepsilon_{Hf}(t)$ values, but low crustal incubation time (Fig. 2), arguing for their probably being derived from a newly formed island arc crust with the direct addition of depleted mantle material. Considering that zircon Lu–Hf analyses for Silurian to Carboniferous granitoids were reported neither in this study nor in previous literature in the Harlik belt, the evolutionary process of the Harlik arc during this period does not rely on Lu–Hf isotope data in the following discussion. From Middle Ordovician to Late Devonian (c. 470–380 Ma) (stage 1), zircons from the Dananhu belt granitoids maintain highly positive $\varepsilon_{Hf}(t)$ values and show a sharp rising trend of the event signature curve, and most of the magmatic zircons have a short crustal incubation time (Fig. 2), indicating an input of juvenile mantle material directly forming the intraoceanic arc crust, which further suggests continuous northward subduction of the Kangguer ocean (trench advance) and progressive maturation of the Dananhu–Harlik arc crust. This inference is reinforced by the onset of Ordovician to Late Devonian volcanic sediment and dioritic to granitic plutons with arc-type features as well as thickening of the Dananhu–Harlik arc crust during this period, proved by selected geochemical indicators, such as the gradual decrease of Ce/Y and Ho/Yb ratios (e.g. Du et al. 2018a; Zhang et al. 2018; Sun et al. 2019).

There was then a magmatic interval from c. 380 to 370 Ma. Later, from the Late Devonian to Early Carboniferous (c. 370–330 Ma) (stage 2), the zircons have positive $\varepsilon_{Hf}(t)$ values, but lower than those from the stage 1 granitoids (Fig. 2a). They show a gradual decrease of $\varepsilon_{Hf}(t)$ values, and display a downward trend with decreasing age of the event signature curve in addition to having a short crustal incubation time (Fig. 2), suggesting they were probably generated by reworking of the juvenile arc crust. The most suitable tectonic background for the reworking of the juvenile arc crust could

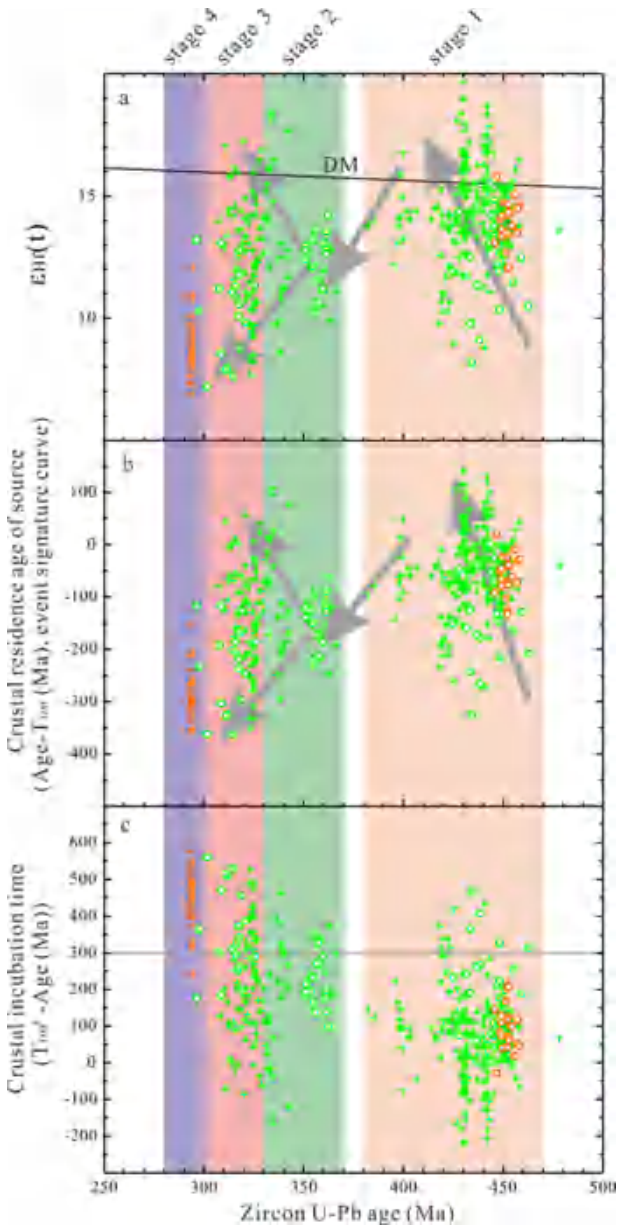

Fig. 2. Plots of Hf isotopic characteristics for magmatic zircons from granitoids in the Harlik belt (red) and Dananhu belt (green); the data represented by circles are from this study (reported inTable S1) and the data represented by crosses are from previous literature (data and references are provided in Table S2). (a) $\varepsilon_{Hf}(t)$ v. zircon U–Pb age, (b) crustal residence age of source v. zircon U–Pb age, and (c) crustal incubation time v. zircon U–Pb age.

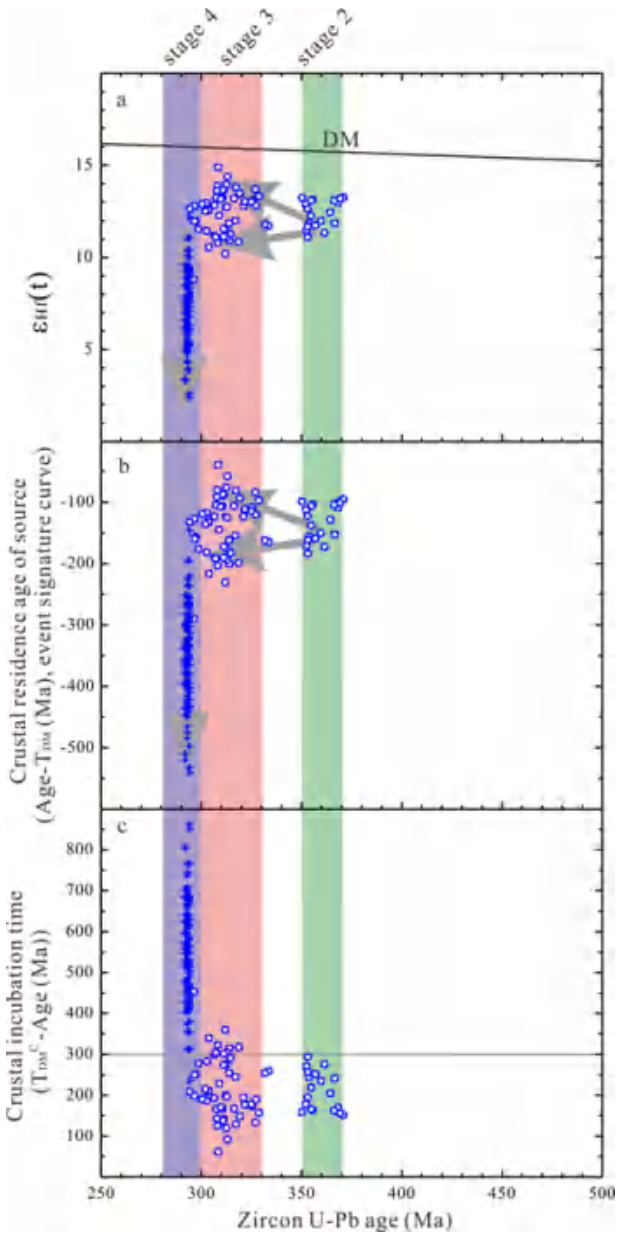

Fig. 3. Plots of Hf isotopic characteristics for magmatic zircons from granitoids in the Kangguer belt; the data represented by circles are from this study (Table S1) and the data represented by crosses are from previous literature (Table S2). (a) $\varepsilon_{Hf}(t)$ v. zircon U–Pb age, (b) crustal residence age of source v. zircon U–Pb age, and (c) crustal incubation time v. zircon U–Pb age.

be the southward rollback of the downgoing Kangguer oceanic plate (trench retreat), which would cause an extension of the overriding Dananhu–Harlik arc crust and possible development of back-arc basins. Located between the Harlik and Dananhu arcs, the earliest strata in the Bogda belt are dominated by littoral–neritic facies clastic sediments and biolimestone with fossil assemblages, which indicate Carboniferous depositional ages (Shu et al. 2011). Furthermore, there are documented extensive Carboniferous bimodal volcanic suites in the Bogda belt, which show both intraplate- and arc-like magmatic affinities, implying that they were associated with an extensional setting and probably represented a back-arc basin (e.g. Chen et al. 2013; Zhang et al. 2017, 2018; Zhu et al. 2020).

Subsequently, from latest Early Carboniferous to Late Carboniferous (c. 329–300 Ma) (stage 3), the zircons from the Dananhu granitoids show large variations in $\varepsilon_{Hf}(t)$ values and have a wide range of crustal residence ages as well as crustal incubation times (Fig. 2). Considering that these zircons have positive $\varepsilon_{Hf}(t)$ values, generation both by addition of juvenile material and reworking of the pre-existing arc crust has been suggested as a possible mechanism for these granitoids. Hence, the renewed northward subduction of the Kangguer ocean (trench advance) is the most likely geodynamic background. This is further supported by the widely developed Late Carboniferous granitoids throughout the Dananhu belt which display typical arc magmatic trace element patterns (e.g. Xiao et al. 2017; Wang et al. 2018; Du et al. 2019a). This model is well supported by the Late Carboniferous (c. 317–302 Ma) adakitic rocks exposed in the north Kangguer belt, which are considered to have been generated by partial melting of the subducted Kangguer oceanic crust (Du et al. 2019b).

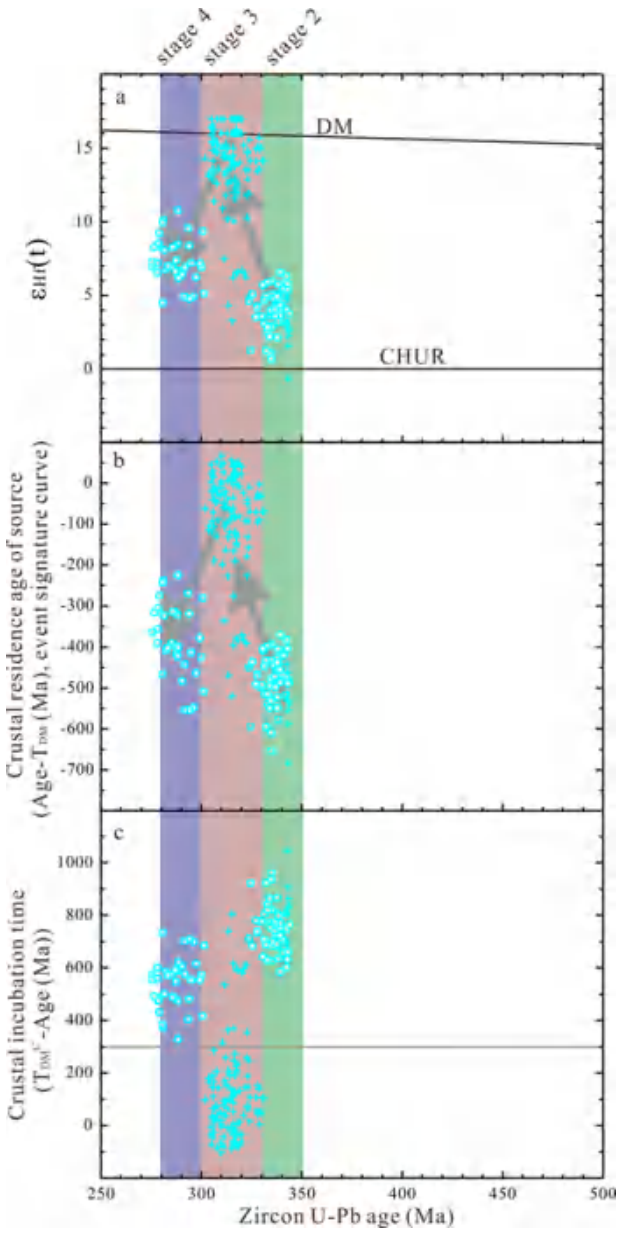

Fig. 4. Plots of Hf isotopic characteristics for magmatic zircons from granitoids in the Yamansu belt; the data represented by circles are from this study (Table S1) and the data represented by crosses are from previous literature (Table S2). (a) $\varepsilon_{Hf}(t)$ v. zircon U–Pb age, (b) crustal residence age of source v. zircon U–Pb age, and (c) crustal incubation time v. zircon U–Pb age.

Late Devonian to Early Permian crustal evolution and tectonic switching of the Kangguer suture belt

The Kangguer belt separating the Paleozoic Dananhu–Harlik arc system to the north (e.g. Zhang et al. 2017, 2018; were the Lower Devonian volcanic sediments and a Late Devonian porphyritic granitic pluton (Du et al. 2018a, were the Lower Devonian volcanic sediments and a Late Devonian porphyritic granitic pluton (Du et al. 2019a) and the Late Paleozoic Yamansu arc to the south (e.g. Du et al. 2018b; Zhao et al. 2019a, b; Long et al. 2020) is characterized as a suture belt with SSZ-type ophiolites barely exposed (Li et al. 2008; Liu et al. 2016). Except for a Late Cambrian (c. 494 Ma) ophiolite suite occurring in this suture belt (Li et al. 2008), the earliest magmatic records were the Lower Devonian volcanic sediments and a Late Devonian porphyritic granitic pluton (Du et al. 2019b). The Late Devonian granites have homogeneous high $\varepsilon_{Hf}(t)$ values, with short crustal incubation times (Fig. 3), implying a young source origin. It is worth noting that the contemporaneous Hf-in-zircon isotopic characteristics of the Kangguer belt granitoids are consistent with those in the Dananhu belt (Figs 2 and 3). Moreover, they display representative island arc-like geochemical signatures and juvenile Nd model ages as well as positive Nd isotopic ratios, similar to the Late Devonian granitoids in the Dananhu belt (e.g. Du et al. 2019b; Sun et al. 2019), indicating they may also have formed by reworking of the juvenile arc crust. More importantly, regarding all the granitoids occurring in the Northeastern Tianshan, the stage 1 granitoids are exposed only to the north of the Dananhu and Harlik belts, whereas the stage 2 granitoids can be observed in the South Dananhu belt, the North Kangguer belt (c. 370–350 Ma), and the Yamansu belt (c. 350–330 Ma), but the stage 3 and stage 4 (Early Permian (c. 299–280 Ma)) granitoids are widely developed throughout the Northeastern Tianshan (e.g. Du et al. 2018a, b, 2019a, b; Sun et al. 2019; Zhao et al. 2019a, b; Long et al. 2020). The above evidence suggests that the Kangguer subducting oceanic slab was southward migrating during this period (c. 370–350 Ma), in accordance with the interpretation for the contemporaneous granitoids in the Dananhu belt.

The distinct distribution range of the granitoids before and after the latest Early Carboniferous (c. 330 Ma) in the Northeastern Tianshan probably reflect a tectonic transition in this area. This was coincident with a magmatic interlude in the Kangguer belt from c. 350 to 330 Ma. In addition, the zircons from the stage 3 granitoids in the Kangguer belt possess a slightly larger variation of $\varepsilon_{Hf}(t)$ values than the earlier granitoids in the same belt, and show an intermediate slope of the event signature curve (Fig. 3). However, they still contain highly positive $\varepsilon_{Hf}(t)$ values with short crustal incubation times, implying they originate from a mixing source.

Nevertheless, the stage 4 granitoids display a significant decrease in $\varepsilon_{Hf}(t)$ values and event signature curve and have long crustal incubation times (Fig. 3), suggesting they are likely to be formed by reworking of the pre-existing juvenile crust. In addition, the geochemistry of many magmatic rocks formed in this stage indicate a post-collisional extensional setting in the Northeastern Tianshan, such as c. 288–284 Ma A-type granites in the Balikun area of the Harlik belt (Yuan et al. 2010), c. 297–295 Ma bimodal volcanic rocks in the Qijiaojing area of the Bogda belt (Chen et al. 2011), c. 287 Ma A-type granites in the Shaerhu area of the Dananhu belt (Mao et al. 2014), and c. 292 Ma A-type granites in the Aqishan mountain of the Yamansu belt (Du et al. 2018b), etc. This is consistent with recent studies on U–Pb ages and Hf isotope analyses of detrital zircons from the early Triassic sandstones in the Dananhu arc, which reveal a provenance from the Yamansu–Central Tianshan arc (Chen et al. 2020). Because detrital zircons can sometimes be derived from sediments within a residual marine basin during or even after collision, the collision timing constrained by them will always be later than the real collision. If the studied detrital zircons were derived from a residual marine basin, the youngest age actually suggests that the Kangguer ocean was closed earlier than the latest Permian–Early Triassic (Chen et al. 2020). This is in good agreement with the collisional and metamorphic timing recorded by gneisses and zircon overrims at 303–301 Ma in the Yamansu belt (Zhang et al. 2016; Du et al. 2018c; Long et al. 2020), as well as the c. 300 Ma shear zone-hosted Au deposits in the Kangguer belt (Xiao et al. 2004), implying that the Kangguer ocean was closed in the latest Carboniferous and the subduction setting probably shifted to a post-collisional background in the earliest Permian (Zhang et al. 2016, 2018; Du et al. 2018b, c; Zhao et al. 2019a, b; Long et al. 2020).

Early Carboniferous to Early Permian crustal evolution and tectonic switching of the Yamansu arc

The earliest magmatic records in the Yamansu belt were formed in the Early Carboniferous, including a calc-alkaline volcanic rock

series in the Yamansu group yielding coeval zircon U–Pb ages of 348 ± 2, 336 ± 2 and 334 ± 3 Ma (Luo et al. 2012), and granodiorites, diorites and albitophyres in the Aqishan area having zircon U–Pb ages of 336 ± 3, 335 ± 2, and 333 ± 3 Ma (Du et al. 2018b). These Early Carboniferous igneous rocks show geochemical features similar to subduction-related magmatic rocks. In addition, the South Tianshan ocean was closed during the Carboniferous based on the 347–320 Ma ages of the eclogites and greenschists from the accretionary wedge in the southern margin of the Central Tianshan block and the South Tianshan terrane (Gao and Klemd 2003; Su et al. 2010). On the other hand, the Central Tianshan block possesses a distinct zircon age cluster around 1400–1600 Ma, which is absent in other nearby Precambrian blocks, such as Tarim in the south, and Tuva–Mongolia in the north (Long and Huang 2017; Chen et al. 2019, 2020). Although we did not find any inherited zircons in our samples, they do occur in the granitic dykes (Long et al. 2020) and volcanic rocks (Luo et al. 2012) in the Yamansu belt which both have a distinct age peak (c. 1400 Ma), and detrital zircons from sandstones in the Southern Kangguer and Yamansu belts have a distinct Proterozoic cluster around 1400–1600 Ma (Chen et al. 2019, 2020). All the above evidence suggests that the Yamansu continental marginal arc was probably associated with southward subduction of the Kangguer oceanic plate instead of northward subduction of the South Tianshan oceanic plate, and the basement of the Yamansu belt is composed of Precambrian basement rocks of the Central Tianshan block (Luo et al. 2012; Du et al. 2018b, c; Chen et al. 2019, 2020; Long et al. 2020). Furthermore, the zircons of the stage 2 granitoids in the Yamansu belt exhibit near-zero $\varepsilon_{Hf}(t)$ values and have the longest crustal incubation times among the Paleozoic granitoids in the Northeastern Tianshan (Fig. 4), indicating that the Precambrian basement of the Central Tianshan block is most likely to be the magma source of these granitoids.

By comparison, the stage 3 granitoids in the Yamansu belt possess highly positive zircon $\varepsilon_{Hf}(t)$ values and display a sharp rising trend of the event signature curve, whereas most of the zircons have a short crustal incubation time (Fig. 4), implying another significant crustal growth event occurred in the Northeastern Tianshan. This crustal growth event is also documented by the whole-rock Nd isotopic data of the Late Carboniferous granitic plutons in this belt, which have highly positive $\varepsilon_{Nd}(t)$ values and juvenile model ages (Zhang et al. 2016; Zhao et al. 2019a, b). During this period, the renewed northward subduction of the Kangguer oceanic plate beneath the Dananhu arc probably drag the southward-subducting slab beneath the Yamansu arc to have a northward rollback, which would cause an extension of the overlying Yamansu arc crust and result in a tectonic transformation into a back-arc basin.

Subsequently, the stage 4 granitoids can be found in Yamansu belt with positive zircon $\varepsilon_{Hf}(t)$ values (Fig. 4a), but significantly lower than those from the stage 3 granitoids. Furthermore, they show a significant decrease in the event signature curve (Fig. 4b), suggesting they were probably generated by a reworking of the pre-existing juvenile crust. Additionally, they have relatively long crustal incubation times (Fig. 4c), supporting that the Yamansu arc crust has contributions from ancient crustal materials. Because the stage 4 granitoids in the Harlik, Dananhu and Kangguer belts also exhibit longer crustal incubation times than those from the earlier stages (Figs 2c and 3c), it is further suggested that the Yamansu granitoids in the stage 4 were formed in the same post-collisional background.

Implications for Paleozoic crustal and tectonic evolution of the Northeastern Tianshan

According to the above discussion, with a formation span of c. 470–280 Ma for the granitoids in the Northastern Tianshan, an integrated crustal and tectonic evolutionary model (Fig. 5) can be proposed to interpret the existing geological observations and the formation of these Paleozoic granitoids.

During stage 1 (Fig. 5a), the initial and continuous northward subduction of the Kangguer oceanic slab resulted in the united Dananhu–Harlik arc system. The trench advance gave rise to the first crustal growth event in the Northeastern Tianshan. The zircons from the granitoids formed during this peroid were characterized by highly positive $\varepsilon_{Hf}(t)$ values and show a sharp rising trend of the event signature curve as well as short crustal incubation times.

During stage 2 (Fig. 5b), the downgoing Kangguer oceanic plate southward rollback caused an extension of the overriding Dananhu–Harlik arc crust, and then developed the Bogda back-arc basin. The trench retreat induced a reworking of the juvenile arc crust in the Dananhu and Kangguer belts. The magmatic zircons in the Dananhu belt and the Kangguer belt granitoids have similar high

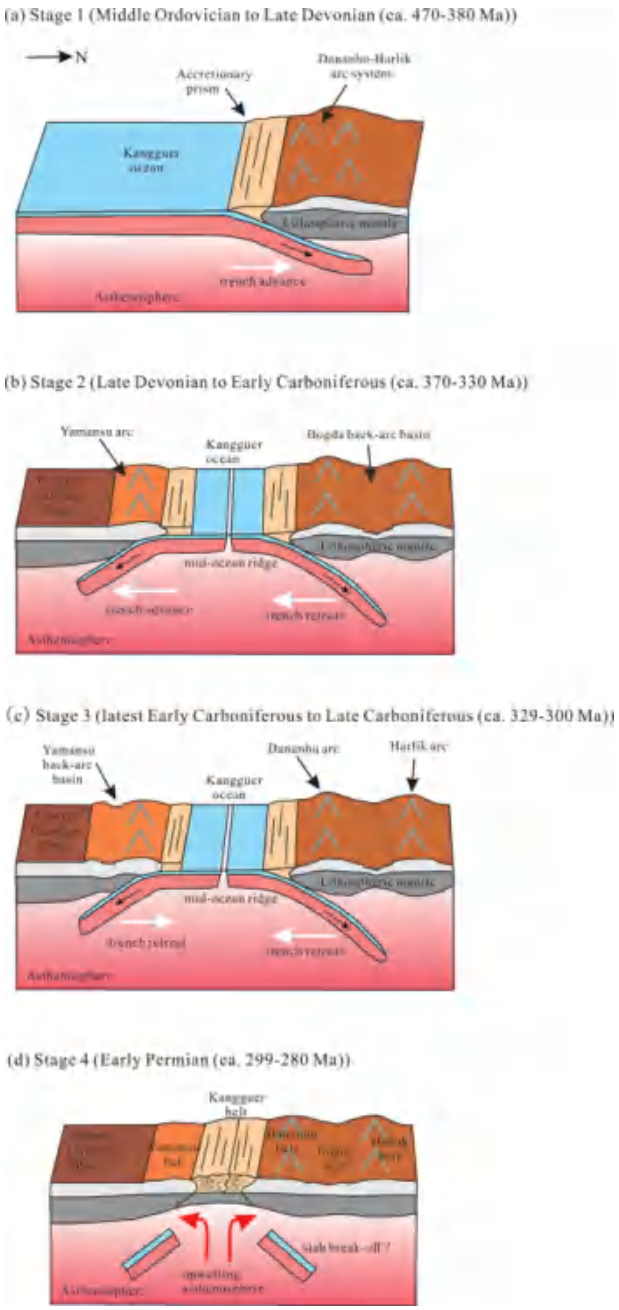

Fig. 5. Schematic diagrams of the Paleozoic evolution of the North Easterneianshan (modified after Zhang et al. 2018).

$\varepsilon_{Hf}(t)$ values and short crustal incubation times. In addition, the zircons from the Dananhu granitoids display a downward trend with decreasing age of the event signature curve. Meanwhlie, the Kangguer oceanic plate began a southward subduction beneath the Central Tianshan block, which produced the Yamansu continental marginal arc. The southern trench advance caused partial melting of the Precambrian basement to generate granitoids with near-zero zircon $\varepsilon_{Hf}(t)$ values and the longest crustal incubation times among the Paleozoic granitoids in the Northeastern Tianshan.

Subsequently, in stage 3 (Fig. 5c), the Kangguer oceanic slab experienced northward migration again, which enhanced the formation of the Dananhu arc (the northern trench advance) and the Yamansu back-arc basin (the southern trench retreat). The granitoids in the Dananhu belt were generated by the interaction of juvenile material addition and pre-existing arc crust reworking. The zircons from these granitoids show large variations in $\varepsilon_{Hf}(t)$ values and have a wide range of crustal residence ages in addition to crustal incubation times. However, the southern trench retreat gave rise to another significant crustal growth event in the Northeastern Tianshan. The zircons from the Yamansu belt granitoids have highly positive $\varepsilon_{Hf}(t)$ values and display a sharp rising trend of the event signature curve with most of the zircons having a short crustal incubation time.

In stage 4 (Fig. 5d), the Kangguer ocean closed and the subduction setting of the Northastern Tiansahn shifted to a post-collisional background. The granitoids formed in this setting were mainly derived from pre-existing juvenile crust reworking, with contributions from ancient crustal materials. The zircons from the stage 4 granitoids in the Harlik, Dananhu, Kangguer and Yamansu belts exhibit a significant decrease in $\varepsilon_{Hf}(t)$ values and event signature curve with long crustal incubation times.

Conclusions

(1) The northern trench of the Kangguer ocean experienced two phases of trench northward advance (c. 470–380 Ma and 329–300 Ma) and an intervening trench retreat (c. 370–330 Ma). Meanwhile, the southern trench of the Kangguer ocean experienced a trench southward advance and a northward retreat at c. 370–330 Ma and 329–300 Ma, respectively.

(2) The trench advance and retreat both induced crustal growth in the Northastern Tianshan, i.e., the northern trench advance at c. 470–380 Ma and the southern trench retreat at 329–300 Ma.

Acknowledgements We thank Yueheng Yang and Le Zhang for their help with the geochemical analyses, and Editor Wenjiao Xiao for his kind editorial help. We are grateful to Xijun Liu and two other anonymous reviewers, whose insightful and constructive reviews greatly improved this manuscript.

Author contributions LD: conceptualization (lead), writing – original draft (lead); HZ: data curation (equal); CY: investigation (equal); YZ: investigation (equal); ZH: investigation (equal); XPL: conceptualization (equal), writing – review & editing (lead); XL: conceptualization (equal), writing – review & editing (lead)

Funding This work was supported by the National Key Research and Development Project (2019YFA0708601), the National Natural Science Foundation of China (41903031 and U1906207), and the China Postdoctoral Science Foundation (2019M652431).

Data availability All data generated or analysed during this study are included in this published article (and its supplementary information files).

Scientific editing by Wenjiao Xiao

References

Belousova, E.A., Walters, S., Griffin, W.L., O'Reilly, S.Y. and Fisher, N.I. 2002. Igneous zircon: trace element composition as an indicator of source rock type. Contributions to Mineralogy and Petrology, 143, 602–622, https://doi.org/10.1007/s00410-002-0364-7

Belousova, E.A., Reid, A.J., Griffin, W.L. and O'Reilly, S.Y. 2009. Rejuvenation vs. recycling of Archean crust in the Gawler Craton, South Australia: evidence from U–Pb and Hf isotopes in detrital zircon. Lithos, 113, 570–582, https://doi.org/10.1016/j.lithos.2009.06.028

Beltrando, M., Hermann, J., Lister, G. and Compagnoni, R. 2007. On the evolution of orogens: pressure cycles and deformation mode switches. Earth and Planetary Science Letters, 256, 372–388, https://doi.org/10.1016/j.epsl.2007.01.022

Boekhout, F., Roberts, N.M.W., Gerdes, A. and Schaltegger, U. 2013. A Hf-isotope perspective on continent formation in the south Peruvian Andes. Geological Society, London, Special Publications, 389, 305–321, https://doi.org/10.1144/SP389.6

Cawood, P.A., Kröner, A., Collins, W.J., Kusky, T.M., Mooney, W.D. and Windley, B.F. 2009. Accretionary orogens through Earth history. Geological Society, London, Special Publications, 318, 1–36, https://doi.org/10.1144/SP318.1

Charvet, J., Shu, L.S. and Laurent-Charvet, S. 2007. Paleozoic structural and geodynamic evolution of eastern Tianshan (NW China): welding of the Tarim and Junggar plates. Episodes, 30, 162–186.

Chen, X.J., Shu, L.S. and Santosh, M. 2011. Late Paleozoic post-collisional magmatism in the Eastern Tianshan Belt, Northwest China: new insights from geochemistry, geochronology and petrology of bimodal volcanic rocks. Lithos, 127, 581–598, https://doi.org/10.1016/j.lithos.2011.06.008

Chen, X.J., Shu, L.S., Santosh, M. and Zhao, X.X. 2013. Island arc-type bimodal magmatism in the Eastern Tianshan Belt, Northwest China: geochemistry, zircon U-Pb geochronology and implications for the Paleozoic crustal evolution in Central Asia. Lithos, 168–169, 48–66, https://doi.org/10.1016/j.lithos.2012.10.006

Chen, Z.Y., Xiao, W.J. et al., 2019. Composition, Provenance, and Tectonic Setting of the Southern Kangurtag Accretionary Complex in the Eastern Tianshan, NW China: implications for the Late Paleozoic Evolution of the North Tianshan Ocean. Tectonics, 38, 2779–2802, https://doi.org/10.1029/2018TC005385

Chen, Z.Y., Xiao, W.J. et al., 2020. Latest Permian–early Triassic arc amalgamation of the Eastern Tianshan (NW China): constraints from detrital zircons and Hf isotopes of Devonian–Triassic sediments. Geological Journal, 55, 1708–1727, https://doi.org/10.1002/gj.3540

Collins, W.J. 2002. Hot orogens, tectonic switching, and creation of continental crust. Geology, 30, 535–538, https://doi.org/10.1130/0091-7613(2002)030<0535:HOTSAC>2.0.CO;2

Collins, W.J., Belousova, E.A., Kemp, A.I.S. and Murphy, J.B. 2011. Two contrasting Phanerozoic orogenic systems revealed by hafnium isotope data. Nature Geoscience, 4, 333–337, https://doi.org/10.1038/ngeo1127

Deng, X.H., Wang, J.B., Pirajno, F., Wang, Y.W., Li, Y.C. and Li, C. 2016. Re–Os dating of chalcopyrite from selected mineral deposits in the Kalatag district in the eastern Tianshan Orogen, China. Ore Geology Reviews, 77, 72–81, https://doi.org/10.1016/j.oregeorev.2016.01.014

Du, L., Long, X.P. et al., 2018a. Early Paleozoic dioritic and granitic plutons in the Eastern Tianshan Orogenic Belt, NW China: constraints on the initiation of a magmatic arc in the Southern Central Asian Orogenic Belt. Journal of Asian Earth Sciences, 153, 139–153, https://doi.org/10.1016/j.jseaes.2017.03.026

Du, L., Long, X.P., Yuan, C., Zhang, Y.Y., Huang, Z.Y., Wang, X.Y. and Yang, Y.H. 2018b. Mantle contribution and tectonic transition in the Aqishan-Yamansu Belt, Eastern Tianshan, NW China: insights from geochronology and geochemistry of Early Carboniferous to Early Permian felsic intrusions. Lithos, 304–307, 230–244, https://doi.org/10.1016/j.lithos.2018.02.010

Du, L., Long, X.P., Yuan, C., Zhang, Y.Y., Huang, Z.Y., Sun, M. and Xiao, W.J. 2018c. Petrogenesis of Late Paleozoic diorites and A-type granites in the central Eastern Tianshan, NW China: response to post-collisional extension triggered by slab breakoff. Lithos, 318–319, 47–59, https://doi.org/10.1016/j.lithos.2018.08.006

Du, L., Yuan, C., Li, X.-P., Zhang, Y.Y., Huang, Z.Y. and Long, X.P. 2019a. Petrogenesis and geodynamic implications of the Carboniferous granitoids in the Dananhu Belt, Eastern Tianshan Orogenic Belt. Journal of Earth Science, 30, 1243–1252, https://doi.org/10.1007/s12583-019-1256-3

Du, L., Zhang, Y.Y., Huang, Z.Y., Li, X.-P., Yuan, C., Wu, B. and Long, X.P. 2019b. Devonian to Carboniferous tectonic evolution of the Kangguer Ocean in the Eastern Tianshan, NW China: insights from three episodes of granitoids. Lithos, 350–351, 105243, https://doi.org/10.1016/j.lithos.2019.105243

Gao, J. and Klemd, R. 2003. Formation of HP–LT rocks and their tectonic implications in the western Tianshan Orogen, NW China: geochemical and age constraints. Lithos, 66, 1–22, https://doi.org/10.1016/S0024-4937(02)00153-6

Gao, J., Qian, Q., Long, L.L., Zhang, X., Li, J.L. and Su, W. 2009. Accretionary orogenic process of Western Tianshan, China. Geological Bulletin of China, 28, 1804–1816 [in Chinese with English abstract].

Gao, J., Klemd, R., Qian, Q., Zhang, X., Li, J.L., Jiang, T. and Yang, Y.Q. 2011. The collision between the Yili and Tarim blocks of the Southwestern Altaids: geochemical and age constraints of a leucogranite dike crosscutting the HP-LT

metamorphic belt in the Chinese Tianshan Orogen. Tectonophysics, 499, 118–131, https://doi.org/10.1016/j.tecto.2011.01.001
Gao, J.F., Zhou, M.F., Qi, L., Chen, W.T. and Huang, X.W. 2015. Chalcophile elemental compositions and origin of the Tuwu porphyry Cu deposit, NW China. Ore Geology Reviews, 66, 403–421, https://doi.org/10.1016/j.oregeorev.2014.08.009
Gerdes, A. and Zeh, A. 2009. Zircon formation versus zircon alteration – new insights from combined U-Pb and Lu-Hf in-situ LA-ICP-MS analyses, and consequences for the interpretation of Archean zircon from the Central Zone of the Limpopo Belt. Chemical Geology, 261, 230–243, https://doi.org/10.1016/j.chemgeo.2008.03.005
Glen, R., Quinn, C. and Xiao, W.J. 2011. Island arcs: their role in growth of accretionary orogens and mineral endowment. Gondwana Research, 19, 567–570, https://doi.org/10.1016/j.gr.2011.01.001
Griffin, W.L., Belousova, E.A., Shee, S.R., Pearson, N.J. and O'Reily, S.Y. 2004. Archean crustal evolution in the northern Yilgarn Craton: U–Pb and Hf-isotope evidence from detrital zircons. Precambrian Research, 13l, 23l–282l, https://doi.org/10.1016/j.precamres.2003.12.011
Griffin, W.L., Belousova, E.A., Walters, S.G. and O'Reilly, S.Y. 2006. Archaean and Proterozoic crustal evolution in the Eastern Succession of the Mt Isa district, Australia: U-Pb and Hf-isotope studies of detrital zircons. Australian Journal of Earth Sciences, 53, 125–149, https://doi.org/10.1080/08120090500434591
Hou, T., Zhang, Z.C., Santosh, M., Encarnacion, J., Zhu, J. and Luo, W.Q. 2014. Geochronology and geochemistry of submarine volcanic rocks in the Yamansu iron deposit, Eastern Tianshan Mountains, NW China: constraints on the metallogenesis. Ore Geology Reviews, 56, 487–502, https://doi.org/10.1016/j.oregeorev.2013.03.008
Hu, A.Q., Jahn, B.M., Zhang, G.X., Chen, Y.B. and Zhang, Q.F. 2000. Crustal evolution and Phanerozoic crustal growth in northern Xinjiang: Nd isotopic evidence. Part I: isotopic characterization of basement rocks. Tectonophysics, 328, 15–51, https://doi.org/10.1016/S0040-1951(00)00176-1
Huang, Z.Y., Yuan, C., Long, X.P., Zhang, Y.Y. and Du, L. 2019. From breakup of Nuna to assembly of Rodinia: a link between the Chinese Central Tianshan Block and Fennoscandia. Tectonics, https://doi.org/10.1029/2018TC005471
Jahn, B.M., Windley, B., Natal'in, B. and Dobretsov, N. 2004. Phanerozoic continental growth in Central Asia. Journal of Asian Earth Sciences, 23, 599–603, https://doi.org/10.1016/S1367-9120(03)00124-X
Kemp, A.I.S., Hawkesworth, C.J., Paterson, B.A. and Kinny, P.D. 2006. Episodic growth of the Gondwana supercontinent from hafnium and oxygen isotopes in zircon. Nature, 439, 580–583, https://doi.org/10.1038/nature04505
Kinny, P.D. and Maas, R. 2003. Lu-Hf and Sm-Nd isotope systems in zircon. Reviews in Mineralogy and Geochemistry, 53, 327–341, https://doi.org/10.2113/0530327
Kröner, A., Kovach, V. et al., 2014. Reassessment of continental growth during the accretionary history of the Central Asian Orogenic Belt. Gondwana Research, 25, 103–125, https://doi.org/10.1016/j.gr.2012.12.023
Kröner, A., Kovach, V., Alexeiev, D., Wang, K.L., Wong, J., Degtyarev, K. and Kozakov, I. 2017. No excessive crustal growth in the Central Asian Orogenic Belt: further evidence from field relationships and isotopic data. Gondwana Research, 50, 135–166, https://doi.org/10.1016/j.gr.2017.04.006
Li, W.Q., Ma, H.D., Wang, R., Wang, H. and Xia, B. 2008. SHRIMP dating and Nd-Sr isotopic tracing of Kanggurtage ophiolite in eastern Tianshan, Xinjiang. Acta Petrologica Sinica, 4, 773–780 [in Chinese with English abstract].
Li, X.H., Li, Z.X. and Li, W.X. 2014. Detrital zircon U–Pb age and Hf isotope constrains on the generation and reworking of Precambrian continental crust in the Cathaysia Block, South China: a synthesis. Gondwana Research, 25, 1202–1215, https://doi.org/10.1016/j.gr.2014.01.003
Liu, W.G., Zhang, J.D. and Zhao, H.L. 2016. Geological Characteristics and geochronology of Dongdagou oceanic crust remmants in Eastern Tianshan, Xinjiang. Western Exploration Engineering, 6, 130–133 [in Chinese].
Long, X.P. and Huang, Z.Y. 2017. Tectonic affinities of microcontinents in the Central Asian Orogenic Belt: a case study of the Chinese Tianshan orogenic belt. Bulletin of Mineralogy, Petrology, and Geochemistry, 36, 771–785 [in Chinese with English abstract].
Long, X.P., Wu, B., Sun, M., Yuan, C., Xiao, W.J. and Zuo, R. 2020. Geochronology and geochemistry of Late Carboniferous dykes in the Aqishane-Yamansu belt, eastern Tianshan: evidence for a post-collisional slab breakoff. Geoscience Frontiers, 11, 347–362, https://doi.org/10.1016/j.gsf.2019.06.003
Luo, T., Liao, Q.A., Chen, J.P., Zhang, X.H., Guo, D.B. and Hu, Z.C. 2012. LA-ICP-MS zircon U–Pb dating of the volcanic rocks from Yamansu Formation in the Eastern Tianshan, and its geological significance. Earth Science - Journal of China University of Geosciences, 6, 1338–1352 [in Chinese with English abstract].
Ma, J.C. 1999. Study on the Huangcaopo Group in the eastern Junggar. Journal of Mineralogy and Petrology, 19, 52–55 [in Chinese with English abstract].
Mao, Q.G., Xiao, W.J. et al., 2014. Geochronology, geochemistry and petrogenesis of Early Permian alkaline magmatism in the Eastern Tianshan: implications for tectonics of the Southern Altaids. Lithos, 190–191, 37–51.
McKenzie, D. and Priestley, K. 2008. The influence of lithospheric thickness variation on continental evolution. Lithos, 102, 1–11, https://doi.org/10.1016/j.lithos.2007.05.005
Meng, Y.K., Xiong, F.H., Yang, J.S., Liu, Z., Lles, K.A., Robinson, P.T. and Xu, X.Z. 2019. Tectonic Implications and Petrogenesis of the Various Types of Magmatic Rocks from the Zedang Area in Southern Tibet. Journal of Earth Science, 30, 1125–1143, https://doi.org/10.1007/s12583-019-1248-3
Royden, L.H., Burchfiel, B.C. and van der Hilst, R.D. 2008. The geological evolution of the Tibetan Plateau. Science, 321, 1054–1058, https://doi.org/10.1126/science.1155371
Scherer, E.E., Whitehouse, M.J. and Münker, C. 2007. Zircon as a monitor of crustal growth. Elements, 3, 19–24, https://doi.org/10.2113/gselements.3.1.19
Sengör, A.M.C., Natalin, B.A. and Burtman, V.S. 1993. Evolution of the Altaid Tectonic Collage and Paleozoic Crustal Growth in Eurasia. Nature, 364, 299–307, https://doi.org/10.1038/364299a0
Shu, L.S., Wang, B., Zhu, W.B., Guo, Z.J., Charvet, J. and Zhang, Y. 2011. Timing of initiation of extension in the Tianshan, based on structural, geochemical and geochronological analyses of bimodal volcanism and olistostrome in the Bogda Shan (NW China). International Journal of Earth Sciences, 100, 1647–1663, https://doi.org/10.1007/s00531-010-0575-5
Smith, P.E., Tatsumoto, M. and Farquhar, R.M. 1987. Zircon Lu-Hf systematics and the evolution of the Archean crust in the southern Superior Province, Canada. Contributions to Mineralogy and Petrology, 97, 93–104, https://doi.org/10.1007/BF00375217
Song, P., Wang, T., Tong, Y., Zhang, J.J., Huang, H. and Qin, Q. 2019. Contrasting deep crustal compositions between the Altai and East Junggar orogens, SW Central Asian Orogenic Belt: evidence from zircon Hf isotopic mapping. Lithos, 328–329, 297–311, https://doi.org/10.1016/j.lithos.2018.12.039
Su, W., Gao, J. et al., 2010. U–Pb zircon geochronology of Tianshan eclogites in NW China: implication for the collision between the Yili and Tarim blocks of the southwestern Altaids. European Journal of Mineralogy, 22, 473–478, https://doi.org/10.1127/0935-1221/2010/0022-2040
Sun, Y., Wang, J.B., Wang, Y.W., Long, L.L., Mao, Q.G. and Yu, M.J. 2019. Ages and origins of granitoids from the Kalatag Cu cluster in Eastern Tianshan, NW China: constraints on Ordovician–Devonian arc evolution and porphyry Cu fertility in the Southern Central Asian orogenic belt. Lithos, 330–331, 55–73, https://doi.org/10.1016/j.lithos.2019.02.002
Tang, M., Wang, X.L., Shu, X.J., Wang, D., Yang, T. and Gopon, P. 2014. Hafnium isotopic heterogeneity in zircons from granitic rocks: geochemical evaluation and modeling of 'zircon effect' in crustal anatexis. Earth and Planetary Science Letters, 389, 188–199, https://doi.org/10.1016/j.epsl.2013.12.036
Tang, G.J., Chung, S.L. et al., 2017. Short episodes of crust generation during protracted accretionary processes: evidence from Central Asian Orogenic Belt, NW China. Earth and Planetary Science Letters, 464, 142–154, https://doi.org/10.1016/j.epsl.2017.02.022
Wang, C.Y., Campbell, I.H., Allen, C.M., Williams, I.S. and Eggins, S.M. 2009. Rate of growth of the preserved North American continental crust: evidence from Hf and O isotopes in Mississippi detrital zircons. Geochimica et Cosmochimica Acta, 73, 712–728, https://doi.org/10.1016/j.gca.2008.10.037
Wang, C.Y., Campbell, I.H., Stepanov, A.S., Allen, C.M. and Burtsev, I.N. 2011. Growth rate of the preserved continental crust: II. Constraints from Hf and O isotopes in detrital zircons from Greater Russian Rivers. Geochimica et Cosmochimica Acta, 75, 1308–1345, https://doi.org/10.1016/j.gca.2010.12.010
Wang, B., Cluzel, D. et al., 2014. Late Paleozoic pre- and syn-kinematic plutons of the Kangguer-Huangshan Shear zone: inference on the tectonic evolution of the Eastern Chinese North Tianshan. American Journal of Science, 314, 43–79, https://doi.org/10.2475/01.2014.02
Wang, Y.F., Chen, H.Y. et al., 2018. Paleozoic tectonic evolution of the Dananhu-Tousuquan island arc belt, Eastern Tianshan: constraints from the magmatism of the Yuhai porphyry Cu deposit, Xinjiang, NW China. Journal of Asian Earth Sciences, 153, 282–306, https://doi.org/10.1016/j.jseaes.2017.05.022
Wang, S.J., Li, X.-P., Duan, W.Y., Kong, F.M. and Wang, Z.L. 2019. Record of Early-Stage Rodingitization from the Purang Ophiolite Complex, Western Tibet. Journal of Earth Science, 30, 1108–1124, https://doi.org/10.1007/s12583-019-1244-7
Windley, B.F., Alexeiev, D., Xiao, W., Kröner, A. and Badarch, G. 2007. Tectonic models for accretion of the Central Asian Orogenic Belt. Journal of the Geological Society, London, 164, 31–47, https://doi.org/10.1144/0016-76492006-022
Xiao, W.J., Zhang, L.C., Qin, K.Z., Sun, S. and Li, J.L. 2004. Paleozoic accretionary and collisional tectonics of the Eastern Tianshan (China): implications for the continental growth of Central Asia. American Journal of Science, 304, 370–395, https://doi.org/10.2475/ajs.304.4.370
Xiao, W.J., Windley, B.F. et al., 2015. A tale of amalgamation of three Permo-Triassic collage systems in Central Asia: oroclines, sutures, and terminal accretion. Annual Review of Earth and Planetary Sciences, 43, 477–507, https://doi.org/10.1146/annurev-earth-060614-105254
Xiao, B., Chen, H.Y., Hollings, P., Han, J.S., Wang, Y.F., Yang, J.T. and Cai, K.D. 2017. Magmatic evolution of the Tuwu–Yandong porphyry Cu belt, NW China: constraints from geochronology, geochemistry and Sr–Nd–Hf isotopes. Gondwana Research, 43, 74–91, https://doi.org/10.1016/j.gr.2015.09.003
Xiao, Z.C., Wang, S., Qi, S.H., Kuang, J., Zhang, M., Tian, F. and Han, Y.J. 2020. Petrogenesis, Tectonic Evolution and Geothermal Implications of Mesozoic Granites in the Huangshadong Geothermal Field, South China.

Journal of Earth Science, 31, 141–158, https://doi.org/10.1007/s12583-019-1242-9

Yuan, C., Sun, M., Wilde, S., Xiao, W.J., Xu, Y.G., Long, X.P. and Zhao, G.C. 2010. Post-collisional plutons in the Balikun area, East Chinese Tianshan: evolving magmatism in response to extension and slab break-off. Lithos, 119, 269–288, https://doi.org/10.1016/j.lithos.2010.07.004

Zhang, W.F., Chen, H.Y., Han, J.S., Zhao, L.D., Huang, J.H., Yang, J.T. and Yan, X.L. 2016. Geochronology and geochemistry of igneous rocks in the Bailingshan area: implications for the tectonic setting of late Paleozoic magmatism and iron skarn mineralization in the eastern Tianshan, NW China. Gondwana Research, 38, 40–59, https://doi.org/10.1016/j.gr.2015.10.011

Zhang, Y.Y., Yuan, C., Long, X.P., Sun, M., Huang, Z.Y., Du, L. and Wang, X.Y. 2017. Carboniferous bimodal volcanic rocks in the Eastern Tianshan, NW China: evidence for arc rifting. Gondwana Research, 43, 92–106, https://doi.org/10.1016/j.gr.2016.02.004

Zhang, Y.Y., Sun, M. et al., 2018. Alternating trench advance and retreat: insights from Paleozoic magmatism in the Eastern Tianshan, Central Asian Orogenic Belt. Tectonics, 37, 2142–2164, https://doi.org/10.1029/2018TC005051

Zhang, X.R., Zhao, G.C., Han, Y.G. and Sun, M. 2019. Differentiating advancing and retreating subduction zones through regional zircon Hf isotope mapping: a case study from the Eastern Tianshan, NW China. Gondwana Research, 66, 246–254, https://doi.org/10.1016/j.gr.2018.10.009

Zhao, L.D., Chen, H.Y., Hollings, P. and Han, J.S. 2019a. Late Paleozoic magmatism and metallogenesis in the Aqishan-Yamansu belt, Eastern Tianshan: constraints from the Bailingshan intrusive complex. Gondwana Research, 65, 68–85, https://doi.org/10.1016/j.gr.2018.08.004

Zhao, L.D., Chen, H.Y., Hollings, P. and Han, J.S. 2019b. Tectonic transition in the Aqishan-Yamansu belt, Eastern Tianshan: constraints from the geochronology and geochemistry of Carboniferous and Triassic igneous rocks. Lithos, 344–345, 247–264, https://doi.org/10.1016/j.lithos.2019.06.023

Zheng, Y.F., Wu, Y.B., Zhao, Z.F., Zhang, S.B., Xu, P. and Wu, F.Y. 2005. Metamorphic effect on zircon Lu-Hf and U-Pb isotope systems in ultrahigh-pressure eclogite-facies metagranite and metabasite. Earth and Planetary Science Letters, 240, 378–400, https://doi.org/10.1016/j.epsl.2005.09.025

Zhu, D.C., Zhao, Z.D. et al., 2011. The Lhasa Terrane: record of a microcontinent and its histories of drift and growth. Earth and Planetary Science Letters, 301, 241–255, https://doi.org/10.1016/j.epsl.2010.11.005

Zhu, H.L., Du, L., Li, X., Zhang, Z.F. and Sun, W.D. 2020. Calcium isotopic fractionation during plate subduction: Constraints from back-arc basin basalts. Geochimica et Cosmochimica Acta, 270, 379–393, https://doi.org/10.1016/j.gca.2019.12.004